INFLUENCE OF HYDROGEN PRESENCE ON FATIGUE BEHAVIOUR OF A VESSEL STEEL

F. Gutiérrez-Solana(*), L. Caballero(**), M.Elices(**) and A.Valiente(**)

This work presents the fatigue behaviour of a ST 52/35 vessel steel, in air and in simulated hydrogen environments at room conditions. Results are compared with SEM fractographic analyses in order to appreciate the influence of hydrogen presence on the fatigue behaviour of this steel.

The obtained results show an important reduction of vessel life in the presence of hydrogen.

INTRODUCTION

The study of safety conditions of gas transport and storage systems is considered very important for engineering, economic and environmental reasons. Fracture Mechanics analyses help in the assessment of these conditions.

The presence of hydrogen in such systems, pure or mixed with other gases, shows the necessity for understanding its effect on the mechanical behaviour of the material usually used in the construction of pipes and vessels, because of the posibility of hydrogen embrittlement.

So, this work analyzes the influence of hydrogen on the fatigue behaviour of a ST 52/35 vessel steel, of composition and mechanical characteristics described in Table 1.

(*) E.T.S. Ingenieros de Caminos. Universidad de Cantabria. Santander Spain
(**) E.T.S. Ingenieros de Caminos. Universidad Politécnica de Madrid. Spain

TABLE 1.- Chemical composition (weight %) and mechanical characteristics of ST 52/35 steel

C	S	P	Si	Mn
0,16	0,04	0,02	0,27	1,45

Ferritic-pearlitic microstructure
Yield strength ..... 365 MPa
Ultimate strength ..... 530 MPa
Strain at max. load ..... 22 %
Fracture toughness. Obtained from J_{IC} test. 103 Mpa $m^{1/2}$

FATIGUE BEHAVIOUR

Two types of test were performed: Standard tests in air and tests in air of samples previously charged with hydrogen.

Air tests

Fatigue test in air at room conditions were done using 12,5 mm. thick compact type specimens, whose stress intensity factor as a function of load, crack length and dimensions is well known. (Brown (1)).

All the fatigue tests were performed with a load ratio, R, of 0.1 and a constant frequency of 30 Hz. All of them were focussed on the determination of the threshold value, ΔK_{th} (stage I), and the crack propagation rate, da/dN (stage II), as a function of ΔK, by defining the Paris law.

Due to the absence of standards (ASTM (2)) covering all the caracterization processes, particularly those related with threshold determination, special considerations have been invoked when analyzing the obtained data in order to optimize their representativity of the material response.

After each reduction in load done in a test to determine the threshold value, a slower crack propagation rate than expected was registered in a zone related to the size of the plastic zone which was stablished before the reduction. When the crack propagates beyond this affected zone, the propagation rate becomes stabilized at values that depend on the corresponding ΔK. Figure I shows this effect by comparing the ratio of measured crack propagation rate, da/dN, to the corresponding stabilized one, (da/dN)*, versus the distance, or crack propagation, measured from the crack front at the time when the reduction in load was done.

From this figure, the crack prpagation rate data, if obtained at a distance from the crack front at reduction, a, which is lower than the value Δa^* as defined in expression (1), are not representative of the material behaviour.

$$\Delta a^* \simeq \frac{1}{\pi}\left(\frac{K^2_{max,b} - K^2_{max,a}}{\sigma_y^2}\right) \qquad (1)$$

where $K_{max,b}$: max. stress intensity factor for the load before the reduction.

$K_{max,a}$: max. stress intensity factor for the load after the reduction.

This effect of an existing plastic zone obligates one to choose low percentages for load reductions, from 5 to 2%, to avoid false threshold values. Figure 2 shows the ΔK-da/dN relation near threshold, for two different samples. The ΔK_{th} value obtained was 9.2 ± 0.7 MPa.$m^{1/2}$ but, as can be seen in Figure 3, the variation can be related to the relative crack length, a/w, at arrest position due to crack closure effects.

The stage II, crack propagation rate zone, was characterized by the Paris law:

$$da/dN = 2.1 \cdot 10^{-14} \Delta K^{4.8} \qquad (2)$$

Figure 4 shows the obtained data used to determine this expression.

Hydrogen tests

To characterize the fatigue behaviour of this steel in hydrogen, the same kind of specimens were cathodically charged in a 1N sulfuric acid solution with 1mA/cm^2 current density. The internal hydrogen embrittlement represents a loss of ductility equivalent to the one produced by the environmental embrittlement of the steel in a pure hydrogen atmosphere at 7 MPa of pressure. (Gutiérrez-Solana (3)).

The samples once charged, were cadmium plated by an electrolitic method, to avoid external hydrogen diffussion. Then, they were tested following the same methodology as those in air. Figure 5 shows the obtained data for stage I with reference to air behaviour. The corresponding threshold values were lower than the air-value, but the differences can be due to the above mentioned influence of crack length at arrest, as can be seen in Figure 6. Hence a clear influence of hydrogen presence over the ΔK_{th} values has not beet observed.

The characterization of crack propagation rate was then imitially evaluated with the same conditions as those in air, 30 Hz of frequency and a constant cyclic load function. Knowing that cyclic frequency has been shown to be an important factor in fatigue crack growth in hydrogen (Gallagher and Wei (4),

Wei and Shim (5)), changes in this variable were continuosly introduced during testing, initially from 30 Hz to 10 Hz and vice-versa and at lower values, 5 and 1 Hz later. From the results obtained changes from lower to higher frequencies should be avoided because these induce an irregular behaviour. Figure 7 shows the complete behaviour obtained in the propagation stage, associated with changes in frequency, and compared to the corresponding response in air.

A deleterious effect of hydrogen on fatigue crack propagation is observed, providing rates 5 to 10 times higher than those in air. This effect, for each frequency, disappears when the crack propagates faster than a critical rate that increases as the frecuency decreses, 3.10^{-8} m/cycle for 30 Hz and 9.10^{-8} m/cycle for 10 Hz.

Considering the propagation rate refered to time, da/dt, the critical rate becames constant, with a value of 9.10^{-7} suggesting that the hydrogen effect on crack propagation is controlled by hydrogen diffusion at the crack tip (Wei (6)). So, once the crack propagates faster than the critical value the hydrogen has no time to affect the crack propagation.

Finally, the crack was propagated to a length equivalent to the maximum stress intensity factor of this steel for the tests conditions, i.e. up to K_{IC}, where fracture happened (stage III). The obtained value of K_{IC}, 47 MPa.$m^{1/2}$, was in good agreement with previous data on the influence of hydrogen in fracture toughness of this and similar steels (Christenson et al (7)), Gutiérrez-Solana and Elices (8)) and showed the important effect of hydrogen in reducing the stress at fracture by a factor of 2.

FRACTOGRAPHY

To better understand the influence of hydrogen on the fatigue behaviour of this steel an analysis of the fracture surfaces was done by scanning electron microscopy (SEM) techniques.

At threshold no clear differences could be observed between those samples tested in air and those tested in hydrogen. Figure 8 shows this situation, with two micrographs, one for each kind of test.

However, the fracture surfaces in the stage II propagation zone showed up clear differences in fracture mode. As an example of this, Figure 9, shows two micrographs of fracture surfaces at similar ΔK values, one for a sample tested in air with a transgranular fracture mode and the other for a sampled charged with hydrogen with a mixed mode of fracture, transgranular and intergranular; here the more brittle intergranular areas

represent an important part of the total area.

Because of the mechanical behaviour observed due to the changes in frequency for samples tested in hydrogen, a methodical fractographic analysis has been done over fracture surfaces to show the deleterious effect of hydrogen associated to a higher presence of intergranular mode of fracture. The captions contained in Figure 10, all of them for a frequency of 10 Hz, show this relation. Caption a shows the fracture surface at a ΔK value of 13 MPa.$m^{1/2}$, where the effect of hydrogen was the highest (Figure 7); caption b belongs to a zone where the corresponding ΔK value was 18 MPa.$m^{1/2}$ and the effect of hydrogen was decreasing as the crack propagated at a rate close to the critical one, and caption c shows the fracture surface at a ΔK of 23 MPa.$m^{1/2}$ where no effect of hydrogen was observed. From a to c the intergranular mode of fracture decreases clearly, and the later is similar to that observed on samples tested in air.

The SEM analysis that the variation of frequency did not influence the fracture mode, when the hydrogen effect, the stress state, and the propagation rate, are similar. In Figure 11, captions a and b compare the fracture surfaces of two close areas, a was tested at 30 Hz and a ΔK of 16 MPa $m^{1/2}$ and b at 10 Hz and 18 MPa.$m^{1/2}$. These show an equivalent effect of hydrogen presence with a propagation rate 5 times that corresponding to air. No fractographic differences can be observed. At the same figure caption c shows an area for a higher stress intensity situation, where the crack propagated at a rate more than one order of magnitude higher at 1 Hz. The fracture appearance indicates a less strained material, with areas of "quasi-cleavage", associated to a faster propagation.

ANALYSIS OF THE RESULTS

This work shows the influence of hydrogen on fatigue behaviour of the pressure vessel steel tested.

The presence of hydrogen for the given test conditions, simulating a pure hydrogen gaseous atmosphere at 7 MPa pressure, originates the following effects by comparison with the behaviour in air:

-Stage I. No clear differences could be found at ΔK_{th} threshold values. Similar fractographs have been observed for samples tested in air and those charged with hydrogen.

-Stage II. Crack propagation rates can be faster in hydrogen than in air by a factor of 10, if frequency is low enough. With reference to time, da/dt, a critical value was determined as 9.10^{-7} m/s, above which hydrogen has no effect.

This critical value can be understand considering that hydrogen diffussion to the more strained zone of the specimen, the crack tip, controls the mechanisms of fatigue in hydrogen that make it different from fatigue in air. When the effect of hydrogen on crack propagation is present, the associated fracture surface shows a mixed intergranular-transgranular mode of fracture different from the transgranular one on aire, offering apparently an easier path for crack propagation than can explain its higher rate values.

-Stage III. The hydrogen presence causes an embrittlement of the steel, and its fracture toughness decreasses by a factor of 2.

CONCLUSIONS

The obtained fatigue behaviour of the vessel steel should be considered on design or safety control calculations of systems susceptible to be in conditions for what hydrogen is deleteriously effective. In such conditions, the increasing crack propagation rate (x10) and the decreasing frature toughness (x2) can determine an important reduction on system life, in comparison to the one determinated at normal conditions, suggesting the necessity of a much better control of defects in the presence of hydrogen.

AKNOWLEDGMENTS

This work has been funded by Butano, S.A. The fatigue tests were performed at the Department of Metallurgical Engineering and Materials Science of Carnegie Mellon University (Pittsburgh). The authors specially thanks the collaboration and support of the Professors of this University I.M. Bernstein and A.W. Thompson.

SYMBOLS USED

R : Load ratio (minimum load/maximum load) at fatigue tests.
ΔK : Variation of stress intensity factor ($MPa.m^{1/2}$).
ΔK_{th} : ΔK at threshold conditions (stage I) ($MPa.m^{1/2}$).
a : Crack length (m).
a/w : Relative crack length.
da/dN : Cyclic crack propagation rate (m/cycle).
da/dt : Crack propagations rate refered to time (m/s).
σ_y : Yield strength (MPa).
K_{IC} : Fracture toughness ($MPa.m^{1/2}$).

REFERENCES

(1) Brown, B.F. "Stress Corrosion Cracking in High Strength Steel and Titanium and Aluminun Alloys". Naval Research Lab. 1972.

(2) A.S.T.M. Standards - E 647-83. Volume 03.01 ASTM Anual book, 1984.

(3) Gutiérrez-Solana, F. "Fragilización por Hidrógeno en Tuberías de Acero". Ph.D. Thesis. Universidad Politécnica de Madrid. Spain, 1981.

(4) Gallagher, J.P. and Wei, R.P. "Corrosión-Fatigue, NACE-2", Proceedings, Storrs Conn. Edited by O. Devereux, A.J. McEvily and R.W. Staehle, NACE. Houston, Tx, 1972, p. 409.

(5) Wei, R.P. and Shim, G. "Fracture Mechanics and Corrosion Fatigue". Technical Report nº 13. Office of Naval Research, 1981.

(6) Wei, R.P. "Fatigue Mechanisms", ASTM. STP 675, American Society for Testing and Materials, 1979, p. 816.

(7) Christenson, D.J. Bernstein, I.M. Thompson, A.W., Danielson, E.S., Elices, M., and Gutiérrez-Solana, F. "Hydrogen Effects in Metals" Proceedings, Jackson Lake, 1980. Edited by I.M. Bernstein and A.W. Thompson, AIME, Warrendale, 1981, p. 997.

(8) Gutiérrez-Solana, F. and Elices, M. "Current Solutions to Hydrogen Problems in Steel". Proceedings, Washington, 1982. Edited by C.G. Interrante and G.M. Pressouyre. ASM, 1982. p. 181.

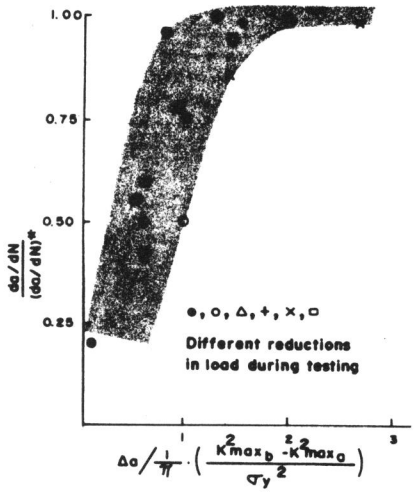

Figure 1.- Effect of load reduction on crack propagation rate.

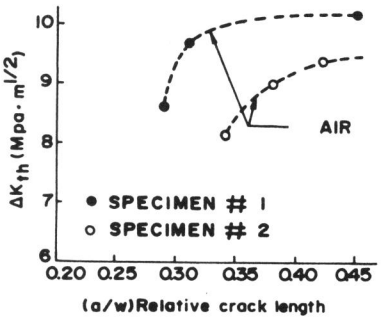

Figure 3.- Effect of relative crack length on ΔK_{th} values

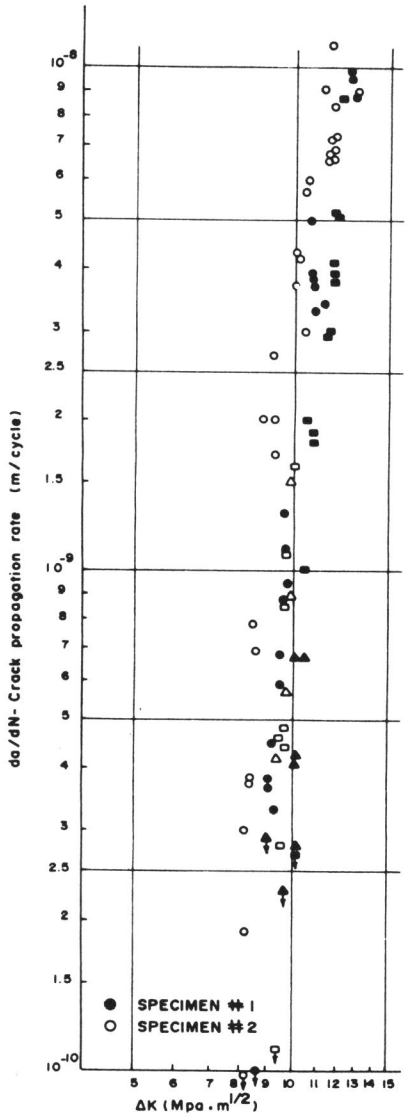

Figure 2.- ΔK-da dN relation near threshold for air fatigue testing

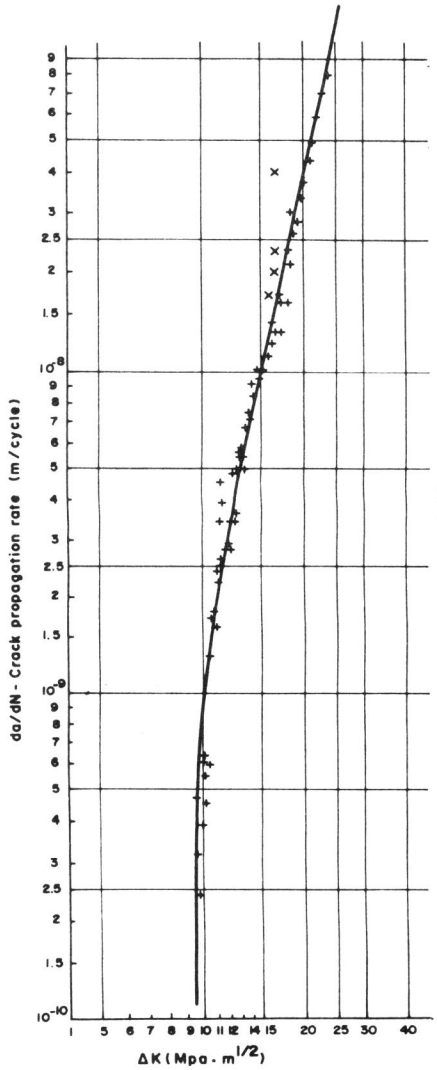

Figure 4.– ΔK-da/dN data in stage II for air fatigue testing.

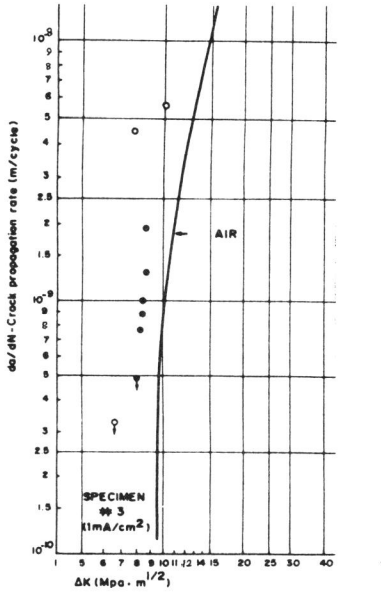

Figure 5.– ΔK-da/dN relation near threshold in the presence of hydrogen

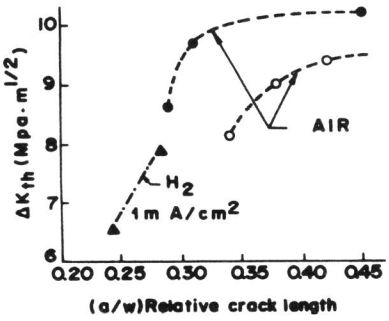

Figure 6.– Effect of relative crack length on ΔK_{th} values for all the samples

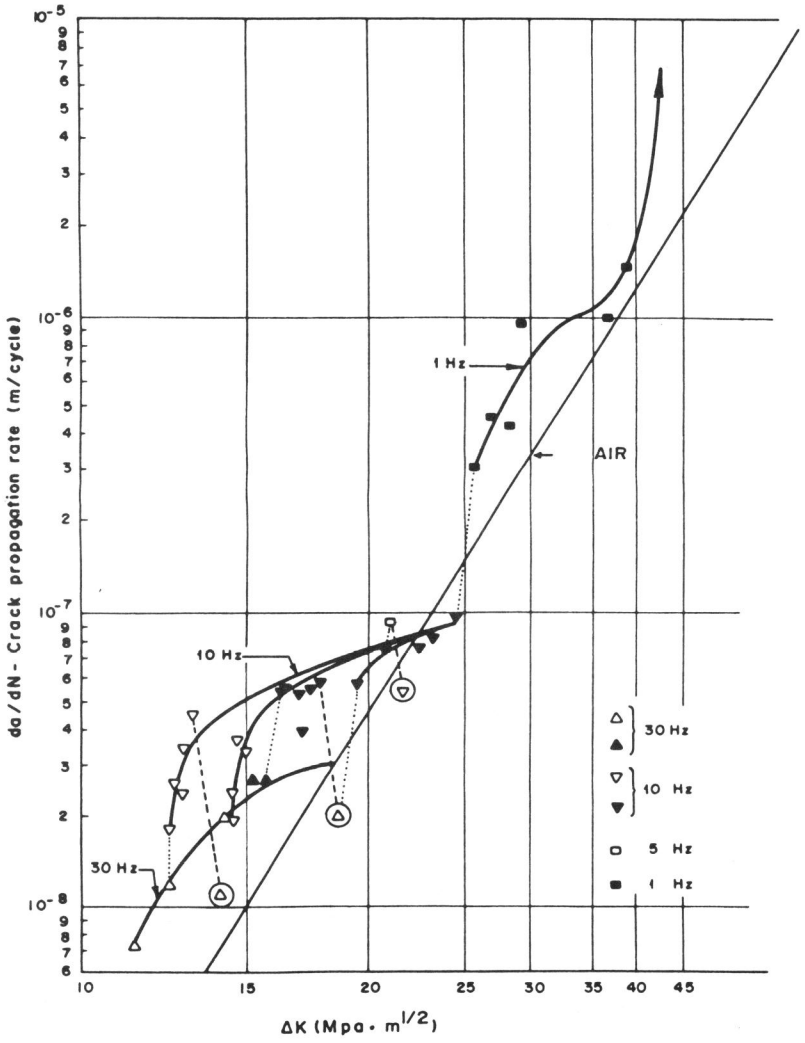

Figure 7.– ΔK–da/dN relation at stage II with hydrogen presence. Influence of different frequencies.

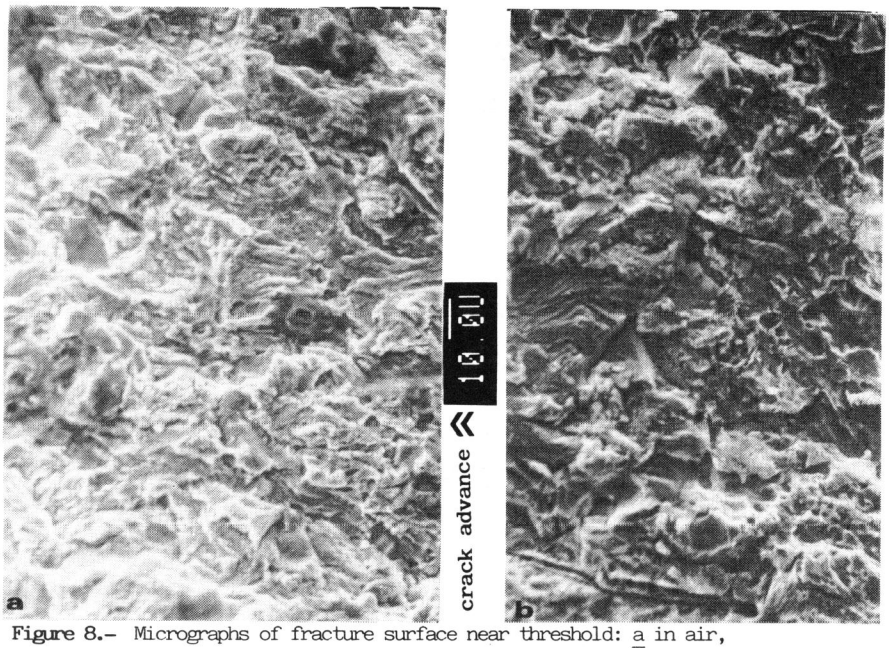

Figure 8.– Micrographs of fracture surface near threshold: a in air, b in hydrogen.

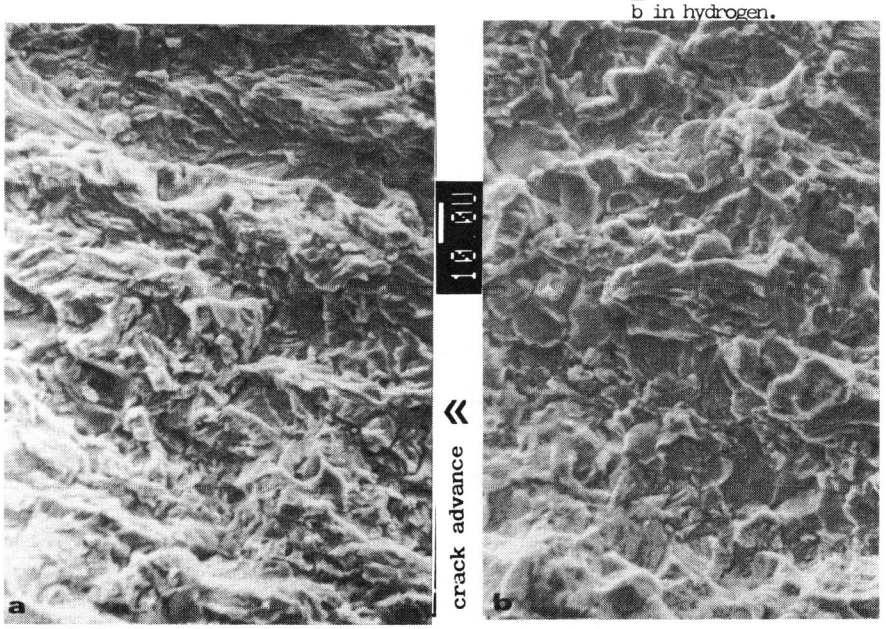

Figure 9.– Micrographs of fracture surface at crack propagation zone (stage II): a in air b in hydrogen

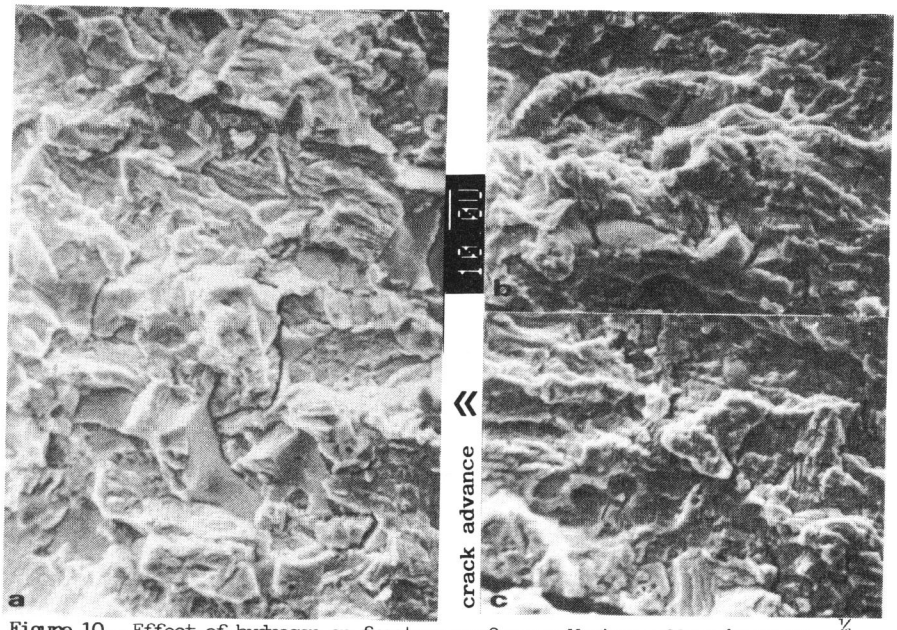

Figure 10.- Effect of hydrogen on fracture surface: a Maximum effect ΔK=13 MPa.m$^{1/2}$
b Intermediate effect ΔK= 18 MPa.m$^{1/2}$ c Non effect ΔK=23 MPa.m$^{1/2}$

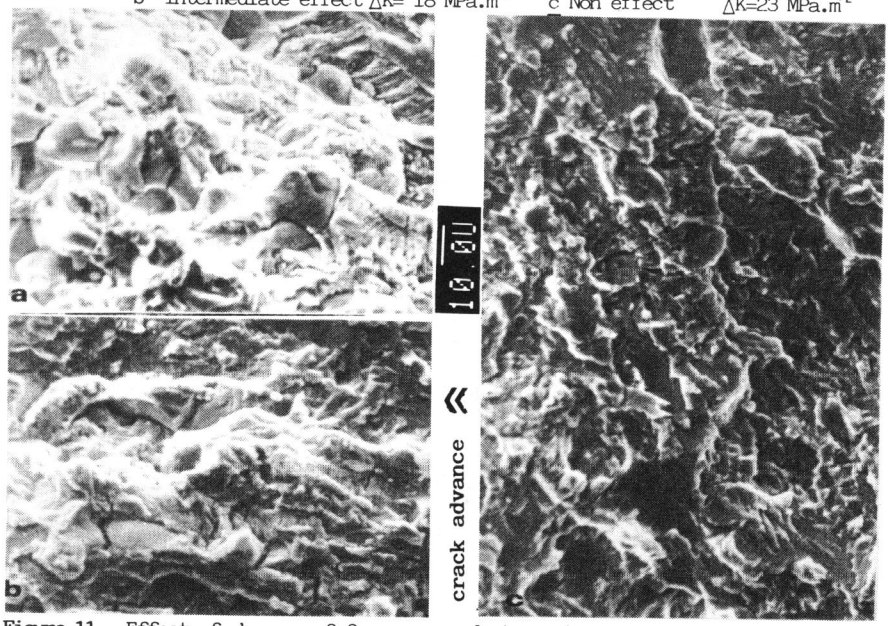

Figure 11.- Effect of changes of frequency and stress intensity on fracture surface:
a 30 Hz, ΔK=16 MPa.m$^{1/2}$ b 10 Hz, ΔK=18 MPa.m$^{1/2}$ c 1 Hz, ΔK=28 MPa.m$^{1/2}$